SWISS NEUTRON NEWS

Number 53 | May 2019

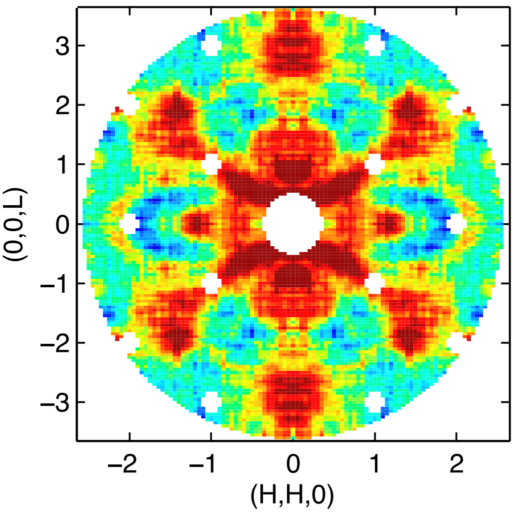

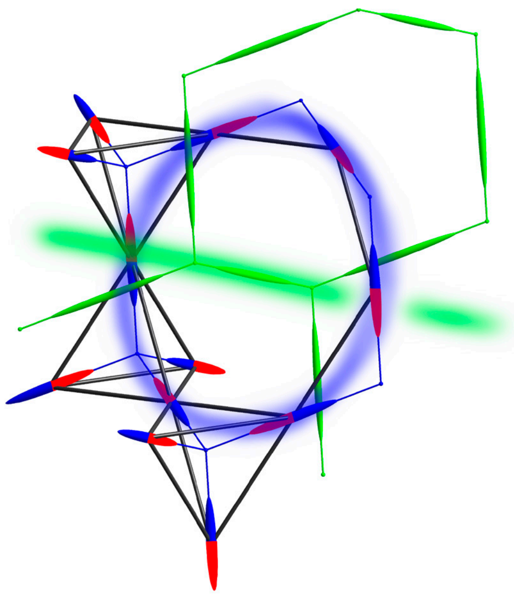

Schweizerische Gesellschaft für Neutronenforschung
Société Suisse de la Science Neutronique
Swiss Neutron Science Society

On the cover

Neutron data of the quasi-elastic structure factor of $Pr_2Hf_2O_7$ (left) and the pyrochlore lattice with magnetic moments shown by ellipses with a six member ring highlighted in blue and the emergent electric flux lines shown in green (right). See the related article "Neutron scattering signatures of a quantum spin ice" by R. Sibille et al.

Contents

The President's Page

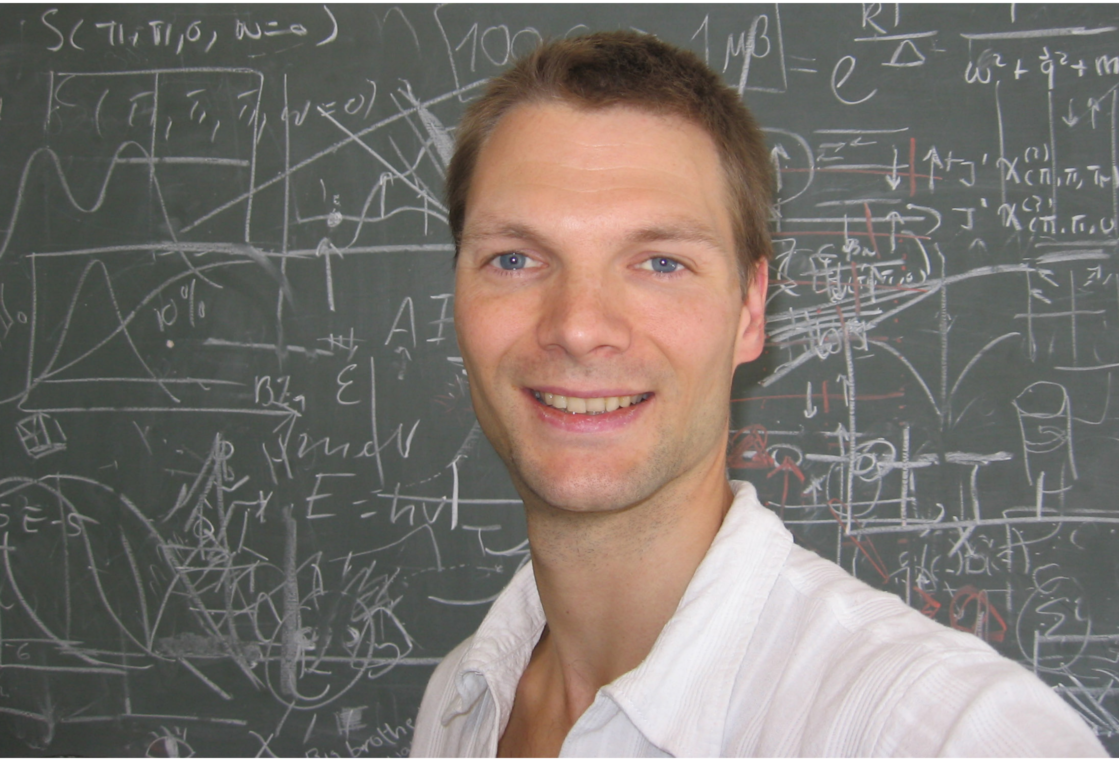

Dear Colleagues,

Welcome to this issue of Swiss Neutron News. You may have noticed the subtle change on the front page – our society is now named Swiss Neutron Science Society – to show that our society represents the interests of all fields of science relying on access to neutron beams. Currently, in 2019, we here in Switzerland have to go abroad for neutron beams. SINQ is on a long shutdown for guide upgrades, which I am informed are proceeding as clock-work – Swiss clock-work of course. We can look forward to significant gains on all instruments in the neutron guide hall once SINQ restarts in 2020. Meanwhile, the vulnerability of the European neutron landscape is evident as never before, with both ILL and FRM2 temporarily off their originally planned cycles – luckily in both cases solutions appear to be close. One important new action is the creation of LENS – League of Advanced Neutron Sources – a consortium to strengthen collaboration and coordination among European neutron user facilities. I believe this is a very important step and believe LENS and ENSA can form an effective partnership that will enhance the efficiency and impact of neutron science.

On the topic of ENSA, we have launched a new prize – the Neutron Instrumentation and Innovation Award. My vision behind this prize is to recognize and reward those scientists who devote their ingenuity and efforts to develop new instruments or methods that benefit the neutron science community. I strongly encourage you to nominate candidates for the prize, which will be awarded at the next European Conference on Neutron Scattering, taking place in St Petersburg June 30th to July 5th, and look forward to meeting many of you there.

Cordially,
Henrik M. Ronnow

New SGN/SSSN/SNSS board members

Markus Strobl

...heads the Neutron Imaging and Applied Materials Group in the Laboratory for Neutron Scattering and Imaging at Paul Scherrer Institute (PSI). After receiving his PhD in Physics from the Technical University Vienna he focused on small angle neutron scattering, neutron reflectometry, neutron imaging and neutron instrumentation at the BER2 reactor of the Helmholtzzentrum Berlin. After 12 years in Berlin he moved to Scandinavia in 2011 to work for the planning and construction of the European Spallation Source as Deputy Head of the Neutron Instrument Division, Instrument Class Coordinator for Engineering Diffraction and Imaging, and Leader of the Engineering, Geoscience and Cultural Heritage Science Focus. He became an affiliated Professor at the Niels Bohr Institute of the University of Copenhagen in 2014 and took his current position in Switzerland in 2017.

Karl W. Krämer

...heads the Solid State Chemistry group at the Department of Chemistry and Biochemistry of the University of Bern. His group investigates rare earth and transition metal halides, their synthesis, crystal growth, optical spectroscopy, and magnetic properties. X-ray and neutron diffraction are used for structural and magnetic studies, inelastic neutron scattering for magnetic excitations. Main research topics are low dimensional quantum magnets, scintillators, and upconversion phosphors. He studied chemistry at Justus-Liebig University Giessen and University of Hannover. After his PhD in 1991 he was postdoc with Prof. H.U. Güdel in Bern, where he became group leader in 2005 and did his habilitation in 2014. [kraemer.dcb.unibe.ch]

LENS

Eight European Partners found the League of advanced European Neutron Sources (LENS).

Representatives of eight European research infrastructures signed the Charter of the **League of advanced European Neutron Sources (LENS)**. The signing ceremony took place at the International Conference of Research Infrastructures, ICRI2018, in Vienna on September 12th and marks the establishment of a new strategic consortium of European neutron sources, which run strong international user programs.

The founding partners in the consortium include both European and national facilities in France, Germany, Sweden, Hungary, the United Kingdom, Norway and Switzerland. Other qualifying facilities are invited to join at any time.

Representatives of the eight founding partners from left to right: Arve Holt (Institute for Energy Technology), Tamás Belgya (Budapest Neutron Centre), Eric Eliot (Laboratoire Léon Brillouin), Helmut Schober (Institute Laue-Langevin), John Womersley (European Spallation Source ESS), Christof Niedermayer (Paul Scherrer Institut), Stephan Förster (Heinz Maier-Leibnitz-Zentrum), Philip King (ISIS Neutron & Muon Source).

The establishment of LENS comes at a moment of transition in European neutron science, and places particular emphasis on the interaction between the neutron science user communities and funding organizations. By optimizing resources and closely aligning policies among partners, the LENS vision is one of continuous improvement and adaptation by neutron source facilities to the communities they serve.

As a centre of competence for neutron scattering in Switzerland the Laboratory for Neutron Scattering and Imaging (LNS) is already involved in scientific and technological collaborations with a number of international neutron facilities. With its strong involvement in the design and building of five different neutron instruments, LNS also contributes considerably to the construction and future operation of the European Spallation Source ESS in Lund in Sweden.

Jean-David Malo from the European Commission emphasized the importance of the LENS consortium for more impactful and open European neutron science and recognized "the LENS consortium objectives to be well aligned with the Long term sustainability plan for Research Infrastructures of the Commission".

For Michel Kenzelmann, Head of the Laboratory for Neutron Scattering and Imaging at PSI, LENS will play an important role towards a healthy neutron landscape in Europe: "Neutron scattering has in the past played an important role towards the development of novel materials for advanced material applications, and this has been recognized by several Nobel Prizes. The increasing demand on materials performance can only be satisfied with the kind of nano- to microscale materials engineering that is possible with neutron scattering and imaging."

Jean-David Malo of the European Commission welcomed the formation of the of LENS consortium.

LENS Founding Members

Budapest Neutron Centre
Hungary

Institute for Energy Technology
Norway

European Spallation Source
Sweden / Denmark

ISIS Neutron & Muon Source
United Kingdom

Heinz Maier-Leibnitz Zentrum
Germany

Laboratoire Léon Brillouin
France

Institut Laue-Langevin
France

Paul Scherrer Institut
Switzerland

Neutron Instrumentation and Innovation Award

of the European Neutron Scattering Association

The inaugural 2019 Neutron Instrumentation and Innovation Award sponsored by Mirrotron.

The European Neutron Scattering Association hereby announce the **inauguration of a new prize**, the **Neutron Instrumentation and Innovation Award**. The prize will be awarded to an early career scientist or engineer in recognition of ground-breaking contributions in neutron instrumentation or method innovation, thereby enabling advances in neutron science and technology. This includes realization of new neutron instruments, pioneering of neutron science in new fields of applications, invention of new neutron techniques or development of new analysis methods and software, as well as other major contributions **enabling advancement of neutron science.** Early career typically means 3-10 years after a PhD, but both younger and more senior candidates may be considered. The prize amount (1 million Hungarian Forints) is generously sponsored by the company Mirrotron, a leading manufacturer of neutron instrumentation components. The Prize will be awarded biennially (synchronized with the European or international Neutron Scattering Conferences).

The inaugural award of the Neutron Instrumentation and Innovation Award will be made at a special ceremony at the European Conference on Neutron Scattering (ECNS 2019), the 1st to 5th July in Saint Petersburg in Russia. The detailed guidelines of the Neutron Instrumentation and Innovation Award are listed on the ENSA web pages (http://www.neutrons-ensa.eu).

Call for Nominations

European scientists as individuals or on behalf of a Division, Section or Group may submit nominations for the 2019 Neutron Instrumentation and Innovation Award of the European Neutron Scattering Association (ENSA). Nominations should include a nomination letter motivating the award, a brief curriculum vitae of the candidate, a description or publication describing the nominated work. Letters of support may be included. Nominations for the Prize will be treated in confidence and although they will be acknowledged, there will be no further communication.

Deadline

Nominations should be sent before **31st of May 2019** to the President of the Selection Committee, preferably by electronic mail in pdf format:

Professor Henrik M. Rønnow
Laboratory for Quantum Magnetism (LQM)
Ecole Polytechnique Federale de Lausanne (EPFL)
1015 Lausanne
Switzerland

Email: henrik.ronnow@epfl.ch

Neutron scattering signatures of a quantum spin ice

Romain Sibille[1], Nicolas Gauthier[2], Han Yan[3], Monica Ciomaga Hatnean[4], Jacques Ollivier[5], Barry Winn[6], Uwe Filges[2], Geetha Balakrishnan[4], Michel Kenzelmann[1], Nic Shannon[3] & Tom Fennell[1]
[1]Laboratory for Neutron Scattering and Imaging, Paul Scherrer Institut, 5232 Villigen PSI, Switzerland, [2]Laboratory for Scientific Developments and Novel Materials, Paul Scherrer Institut, 5232 Villigen PSI, Switzerland, [3]Okinawa Institute of Science and Technology Graduate University, Onna-son, Okinawa 904-0495, Japan, [4]Physics Department, University of Warwick, Coventry, CV4 7AL, UK, [5]Institut Laue-Langevin, CS 20156, F-38042 Grenoble Cedex 9, France, [6]Quantum Condensed Matter Division, Oak Ridge National Laboratory, Oak Ridge, Tennessee, USA, *email: romain.sibille@psi.ch

After R. Sibille *et al*. Nature Physics **14**, 711-715 (2018)

Quantum spin ice is an appealing proposal of a quantum spin liquid – systems where the magnetic moments of the constituent electron spins evade classical long-range order to form an exotic state that is quantum entangled and coherent over macroscopic length scales. Such phases are at the edge of our current knowledge in condensed matter as they go beyond the established paradigm of symmetry-breaking order and associated excitations. Neutron scattering experiments on the pyrochlore material $Pr_2Hf_2O_7$ reveal signatures of a quantum spin ice state that were predicted by theory.

INTRODUCTION

Water in its solid form is a peculiar phase of condensed matter: hydrogen atoms occupy the space between tetrahedrally coordinated oxygen atoms, and each oxygen obeys a local rule of forming two long and two short distances with neighbouring hydrogens. This 'ice rule' prevents crystalline water from selecting a single, unique configuration of hydrogen bonds. Instead, water is characterized by a manifold of classical ground states, whose extent just grows exponentially with the sample size. The existence of this manifold of states amounts to a sort of randomness, so that water ice has a 'residual entropy' near zero temperature, which was first realized by Pauling [1] and is of course an interesting fundamental question in the context of the third law of thermodynamics. In spin ices [2], atoms in their lattices are arranged in geometries that resemble that of frozen water, and an analogous local rule for the electronic spins also prevents the formation of a single state of minimal energy – hence the name spin ice.

Discovered in the late 90s in rare-earth pyrochlore oxides, (dipolar) spin ices are materials that contain large magnetic moments distributed on a network of corner-sharing tetrahedra (about 10 μ_B in the case of Ho^{3+}). The structure of the material, via the crystal electric field acting at the rare-earth site, constrains each magnetic moment to align along the local trigonal direction joining its position and the centres of two tetrahedra. The interactions between those large magnetic moments are governed by classical dipole-dipole interactions, which turn out to be effectively ferromagnetic between first neighbours and essentially self-screened on larger pair distances. Such a system – uniaxial magnetic moments that are constrained to their local trigonal direction and interact ferromagnetically on a pyrochlore lattice – has an exact mapping with the problem of hydrogen bonds in water ice. In other words, two of the four magnetic moments in each tetrahedron must be oriented inward and the two others outward. As for water, this '2-in-2-out' local constraint can be achieved in a number of ways that grows exponentially with the number of tetrahedra involved, so that no magnetic order can occur. A spin ice is therefore better viewed as a fluctuating fluid — a spin liquid — of correlated moments, despite its name being inherited from a form of crystalline water ice.

Under certain circumstances, spin liquids – including spin ices – retain dynamic fluctuations between degenerate states even at zero temperature, in which case they are collectively defined as quantum spin liquids [3-4]. This important class of states where the electronic spins lack symmetry-breaking magnetic order has long attracted substantial interest from theorists and experimentalists alike, as they harbour a wealth of exotic physics. Although the initial idea traces back to Anderson's 1973 proposal [5], in which valence bonds between neighbouring spins pair into singlets and resonate on the lattice, the definition of a quantum spin liquid has evolved with years. Such states are now better defined by invoking the long-range entanglement of their ground state wavefunction and the fractionalization of their excitations. In other words, singlets of Anderson's proposal would now form at all pair distances, and excitations can be defined as quasiparticles that cannot be constructed as combinations of the elementary constituents of the system. For instance, the excitations of antiferromagnetic spin-half ($S = 1/2$) chains are deconfined spinons, each carrying $S = 1/2$ – fractionalized quasiparticles that are fundamentally different to the $S = 1$ magnons of conventional three-dimensionally ordered magnets. Neutrons can only excite a pair of spinons, which then propagate on the lattice, so that the existence of such fractionalized excitations leads to a continuum of magnetic excitations in a neutron scattering experiment. A famed example in one dimension is $KCuF_3$ [6]. The physics of fractionalization is also visible in two-dimensional magnets, e.g. kagome-lattice $ZnCu_3(OD)_2Cl_2$ [7], honeycomb-lattice α-$RuCl_3$ [8]

and triangular-lattice $YbMgGaO_4$ [9]. In each of these materials, the topology plays a fundamental role in the stabilization of an exotic state of matter, as can be directly inferred from their low dimensionalities and lattice names. In three dimensions, precise predictions of quantum spin liquid states exist – such as the quantum spin ice [10] – but experimental realizations remain rather elusive.

FROM "COULOMB PHASE" TO "MAXWELL PHASE"

Magnetic moments in a spin ice can be seen as local magnetic fluxes B_i that link to form a diamond lattice (Figure 1). The ice rule constrains the sum of the fluxes at each vertex to remain zero. This description based on spin variables can be transformed to a 'continuous medium' by considering the mean value B(r) of the lattice fluxes over a certain volume (volume centred on r, and much bigger than a lattice constant but much smaller than the size of the system). The vector field B(r) obtained from this 'coarse-graining' operation has the physical meaning of a magnetization. Finally, the zero-divergence condition of the local ice rule implies for the vector field that $B(r)=\nabla\times A(r)$, where the vector potential A(r) is an emergent (Coulomb) gauge field. In other words, the magnetic field emerging from the spin ice manifold has the properties of a Coulomb potential.

The description of spin ices in terms of an emergent 'magnetic Coulomb phase' [11] explains, by itself, their originality and beauty among other phases of condensed matter. It also turns out that this approach describes accurately many aspects of their properties. A celebrated example of exotic behaviour in spin-ice materials is that of magnetic monopoles [12]. The magnetic moments in the material interact in such a manner that separate mag-

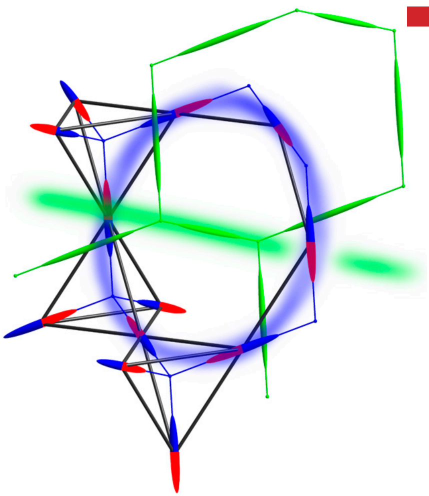

Figure 1
In a classical spin ice (CSI), uniaxial magnetic moments decorate a pyrochlore lattice (in black). Magnetic moments (blue/red ellipses) on each tetrahedra are constrained by a local '2-in-2-out' organization principle. Moments can be viewed as magnetic fluxes forming a diamond lattice (in blue), which can be coarse-grained to define a continuous medium with emergent magnetostatics. Quantum dynamics on a six-member ring create electric flux variables (in green) that form a second (interpenetrated) diamond lattice. This quantum spin ice (QSI) ground state can be thought of as a lattice analogue of quantum electrodynamics – making the sample a tiny universe with its own emergent light of gapless magnetic excitations.

netic charges can emerge as 'quasi-particles' associated with excitations. But exotic as these phenomena may be, they can be still fully described with the framework of classical magnetostatics described in the previous paragraph.

An intriguing question is what happens when quantum effects are thrown into the mix [10]. Theoretical works have predicted that quantum-mechanical tunnelling between different spin-ice configurations can lead to excitations that are qualitatively different from those in classical spin ice (CSI) [13]. In the latter case, the quasi-particles associated with the excitations can be thought of as magnetostatic charges. In contrast, in quantum spin ice (QSI), behaviour emerges that is described by quantum electromagnetism. That is, time fluctuations of the gauge field A(r) give rise to an electric field, E(r), so that the emergent field is now a dynamic electromagnetic field. In a more intuitive 'spin language', the dominant tunnelling processes responsible for the time fluctuations of the spin ice manifold are six-member loops – the centre of which define electric flux variables forming a second, interpenetrated diamond lattice (Figure 1). This leads to a rich set of novel phenomena: not only should quantized variants of magnetic monopoles appear in quantum spin ices, but also electric monopoles (equivalent to electric charges) and excitations that behave like photons.

The experimental realisation of a QSI, however, is challenging, and attempts to identify its manifestations have been made in various pyrochlore materials [14]. Nonetheless, spectacular results of neutron scattering experiments hinting at ground states with quantum origins in rare-earth pyrochlores were thereby obtained over the past few years (see [15-16], for example).

SIGNATURES IN NEUTRON SCATTERING

The free energy of the effective vector field describing a CSI manifold has the form $\mathcal{S} \propto \int d^3\boldsymbol{r}\,\mathcal{B}(\boldsymbol{r})^2$, from which the correlation function can be worked out and written as $\langle S_\mu(-\boldsymbol{k}) S_\nu(\boldsymbol{k})\rangle \propto (\delta_{\mu\nu} - \frac{k_\mu k_\nu}{k^2})$. An important consequence for scattering experiments is the existence of special points in k-space, where the limit depends on the direction of approach. These 'pinch-points' are thus singular features directly originating in the two-in-two-out correlations of the ice rule, and are found in a subset of zone centers. Another remarkable point that can be drawn from this correlation function is the dependence in real space of the spin-spin correlations, $C^B_{\mu\nu}(\boldsymbol{r}) \propto \frac{1}{r^3}$, which is not usual for a liquid.

In the case of classical dipolar spin ices such as $Dy_2Ti_2O_7$ and $Ho_2Ti_2O_7$, however, pinch points proved surprisingly difficult to observe. The reason is the scale of the dipolar interactions present. In classical spin ices, correlations are driven by the interplay of single-ion anisotropy and long-range dipolar interactions, and the latter overlay the pinch points with other, highly-structured, scattering which obscures the pinch-point singularity. Ultimately, pinch points were resolved in $Ho_2Ti_2O_7$, through a carefully-tailored application of polarization analysis [17]. These experiments were specifically designed to separate pinch points in the "spin-flip" (SF) channel from the other, non-singular features arising from dipolar interactions in the "non spin-flip" (NSF) channel.

In contrast, in models of CSI driven by nearest-neighbor exchange interactions alone, polarization analysis is not needed to resolve pinch points. And, as Figure 2 shows [18], pinch points can be cleanly resolved in quasi-elastic scattering from $Pr_2Hf_2O_7$ without any need for polarization analysis, which argues strongly against the presence of dipolar interactions. This is expected given the amplitude of the magnetic moments in this compound, about 2.4 μ_B [19], so that the scale of the dipole-dipole interaction – proportional to the squared moment – reduces to less than 0.1 K, to be compared with about 1.4 K for dipolar spin ices such as $Ho_2Ti_2O_7$. The implication is that the correlated regime appearing below 0.5 K in $Pr_2Hf_2O_7$ [19] must be driven by nearest-neighbour exchange interactions.

We now come to the point of distinguishing between the correlations of a CSI driven by nearest-neighbour exchange interactions and those of an additionally quantum-entangled state such as the QSI model [20-21]. In the latter case, the ground state is governed by the Maxwell action $\mathcal{S} \propto \int dt d^3\boldsymbol{r}\,[\mathcal{E}(\boldsymbol{r})^2 - c^2\mathcal{B}(\boldsymbol{r})^2]$, where c is the speed of light of the emergent photon excitation – a transverse fluctuation of the gauge field. The fact that the spins now fluctuate in time as well as in space introduces an additional power of k in the correlation function, which becomes $\langle S_\mu(-\boldsymbol{k})S_\nu(\boldsymbol{k})\rangle \propto k(\delta_{\mu\nu} - \frac{k_\mu k_\nu}{k^2})$. At zero temperature this has the effect of eliminating the pinch points [20]. These, however, were also predicted to be partially restored at finite temperatures in a QSI, and a crossover to a CSI regime is expected at higher temperatures [21]. In $Pr_2Hf_2O_7$, we have carefully analyzed the shape of the pinch points in order to attempt to classify the correlated regime on this temperature scale (Figure 3). It turns out that the line-shape of the pinch point scattering

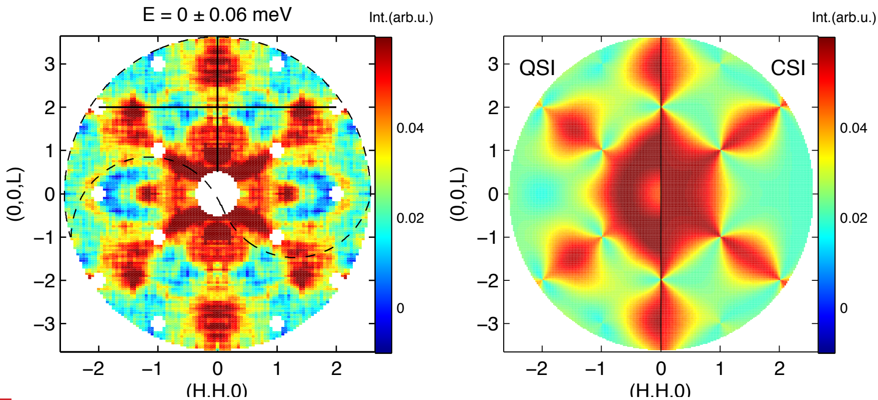

Figure 2
The quasi-elastic structure factor of $Pr_2Hf_2O_7$ measured at 0.05 K on IN5 at ILL (left), and the corresponding patterns calculated using a field theory for the classical nearest-neighbour spin ice (CSI) and quantum spin ice (QSI) models [18]. The two calculated patterns are the correlation functions (including the gapless inelastic scattering of the photon excitations) obtained from the best fits to the line-shape of the pinch point scattering around (0,0,2) – as shown in Figure 3.

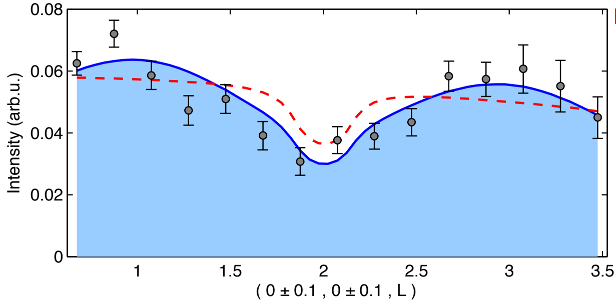

Figure 3
Line-shape of the quasi-elastic structure factor of $Pr_2Hf_2O_7$ measured at 0.05 K on IN5 (grey points with error bars), and the corresponding best fits obtained using a field theory for the classical nearest-neighbour spin ice (CSI – red dashed line) and quantum spin ice (QSI – blue line) models [18].

in our experiment is more consistent with $Pr_2Hf_2O_7$ being in the QSI regime at finite temperature than in a nearest-neighbour CSI regime. Another implication of using the field theory of a QSI to model our data, is that the speed of the emergent light can be directly obtained from the fit of the line-shape of the pinch points. It gives a modest 3.6 meters per second, which – besides being the pace of a 4-hour marathon – translates into a bandwidth of 0.01 meV for the corresponding gapless excitations in a neutron scattering experiment. This bandwidth validates a posteriori our analysis, since the quasi-elastic data shown on Figure 2 integrate over ±0.06 meV and the QSI correlations calculated using the field theory contain the photon excitations.

The QSI model is clearly favoured over the CSI model from the fits of the quasi-elastic scattering (Figure 3). However, the statistical difference does not allow to make a definitive conclusion. In order to confirm that the QSI model explains the ground states properties, we have looked at the inelastic scattering at higher energies, which allows to distinguish between QSI and CSI. Indeed, non-dispersing quasiparticle excitations with a unique energy are the only excitation expected from the monopoles in a CSI, while it is well-established that a continuum of scattering is expected from the quantum-coherent quasiparticles of a QSI (gapped magnetic/electric monopoles). The spectrum presented on Figure 4a reveals a broad continuum of excitations present at 0.05 K, whose magnetic origin is assessed by the polarized neutron spectrum (Figure 4b).The latter was recorded on the HYSPEC spectrometer at Spallation Neutron Source (Oak Ridge National Laboratories, USA), using an array of polarization analysers built at the Paul Scherrer Institut (Villigen, Switzerland). The energy spectra taken in the IN5 data confirm that this continuum of spin excitations extends up to at least E = 1 meV – almost an order of magnitude larger than the dominant exchange in the system, which agrees with theoretical predictions [22-24]. At low energy, the spectral weight is peaked around E = 0.2 meV, which is consistent with our data taken on a powder sample at the same temperature [19]. We also notice that the continuum of scattering is qualitatively similar to recent estimates of the spinon contribution to the local dynamical susceptibility [25]. Importantly, the form of scattering found at finite energy in our data (i.e. the

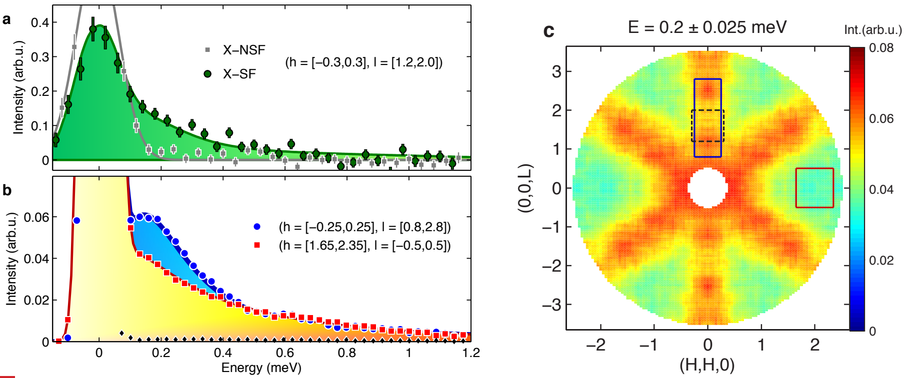

Figure 4

Inelastic spectra of $Pr_2Hf_2O_7$ measured at 0.05 K on HYSPEC using polarized neutrons (a) and on IN5 using unpolarized neutrons (b) [18]. The fact that spin flip scattering of neutrons polarized in the horizontal plane (X-SF) is a purely magnetic signal rules out the possibility that these excitations have a non-magnetic origin. The different spectra for the two integration areas in the IN5 data (blue and red rectangles on panel c) reflect the momentum-space dependence of the excitations that show a “starfish” pattern for energy transfers centred around 0.2 meV (panel c).

“starfish” pattern shown on Figure 4c) differs significantly from the scattering of the quasi-elastic map (Figure 2). The “starfish” scattering at finite energy transfers is highly reminiscent of quantum Monte Carlo simulations for QSI at temperatures where there is a finite density of spinons [26].

MICROSCOPIC ORIGINS

So far, we have essentially described neutron scattering data and compared these with the predictions of a field theory [21], which – by nature – ignores the microscopic details leading to the QSI state. Thus, we now discuss the possible origins of the quantum fluctuations in $Pr_2Hf_2O_7$.

In most rare-earth pyrochlore oxides, at low temperature, the crystal-electric field ground-state doublet is well isolated from the excited levels, so that theoretical models of correlated phases in these materials consider a system of pseudo-spins with S = ½ [27-28]. Given the symmetry at the rare-earth site (D_{3d}), and depending on the number of f electrons and details of the crystal field, the components of the pseudo-spin can have different properties [14]. In the local trigonal direction of the pseudo-spin (i.e. the direction of the magnetic moments that we defined at the beginning for a classical spin ice), the component of the pseudo-spin always transforms like a magnetic dipole. However, in some cases, components in the other directions transform like electric quadrupoles or magnetic octupoles. It was established by theoreticians that interactions between these higher-rank multipoles can stabilize a QSI [29]. This comes with the condition that multipoles act as a transverse perturbation relative to a dominant ferromagnetic interaction establishing the spin ice manifold. In $Pr_2Hf_2O_7$, we have shown in a previous work that the crystal-electric field around the non-Kramers Pr^{3+} ion promotes a ground-state doublet with a magnetic moment along the trigonal direction, and electric quadrupoles in the plane perpendicular to it [19]. It is therefore likely that transverse exchange interactions between quadrupoles play a role in the correlated ground state of this material.

However, multipolar exchange is not the only way to introduce transverse fluctuations in a material like $Pr_2Hf_2O_7$. In pyrochlores, the ground state of a non-Kramers ion such as Pr^{3+} is doubly-degenerate for reasons of crystal symmetry, but this degeneracy can be lifted by structural distortions. Theoreticians have used this to demonstrate that small amounts of non-magnetic disorder in non-Kramers spin ices – equivalent to a random transverse field – is able to turn a CSI into a QSI ground state [30-31]. Therefore, although samples appear to be of very high quality [32], minute amounts of disorder – as always present in real materials – could in fact help stabilizing a QSI ground state in $Pr_2Hf_2O_7$.

Having all these elements in mind, it makes sense to discuss here the origin of the continuum of excitations measured in $Pr_2Hf_2O_7$. Magnetic monopoles cannot usually be excited by scattering neutrons from a non-Kramers ion such as Pr^{3+} [33]. However, magnetic monopoles could be introduced where some sort of residual disorder mixes the dipolar and quadrupolar components of the ground state. The continuum observed in our experiments could also originate in the dual, electric charges of the gauge theory, as was suggested in a recent theory work [33]. Finally, one should note here as well that there are other possible explanations regarding the origin of the observed continuum, which we have considered but could be ruled-out – as stated in more details in our original paper [18].

COMPARISON WITH OTHER PYROCHLORE MATERIALS

The existence of “quantum effects” in pyrochlore materials is not limited to the theoretical understanding and experimental search for the QSI state. Other examples include materials such as, for instance, $Er_2Ti_2O_7$ – where quantum fluctuations may play a role in the ‘order by disorder’ mechanism [34-36]; $Yb_2Ti_2O_7$ – where an exotic long-range order retains dynamics down to the lowest temperatures [28,36-38]; or $Nd_2Zr_2O_7$ – where a peculiar ratio of exchange interactions between different pseudo-spin components leads to the fragmentation of the degrees of freedom into a fluctuating Coulomb phase and a long-range ordered phase of crystallized monopoles [15-16,39].

Different pyrochlore materials based on non-Kramers rare-earths were extensively studied with the aim to find evidence for a QSI ground state. The most studied cases are $Tb_2Ti_2O_7$ and $Pr_2Zr_2O_7$.

$Tb_2Ti_2O_7$ has a rich physics [40-43] where the lattice strongly couples to a spin system that lacks the magnetic long-range order predicted at around 1 K for this Ising antiferromagnet. Recent experiments suggest that electric quadrupole-ordered phases compete with spin liquid ground states depending on the exact stoichiometry of the sample [44-46].

$Tb_2Ti_2O_7$ remains an interesting candidate for the QSI state, whose origin might be related to quantum-mechanical processes allowed by a low-lying crystal-electric field level found around 1 meV [47].

$Pr_2Zr_2O_7$ is the pyrochlore material that is of course most closely related to our study. Tetravalent Zr and Hf cations are indeed quite close in terms of electronegativities and ionic radii, so that the corresponding Pr-based pyrochlore phases might be expected to have the same properties. However, hafnium oxides are even more refractory materials than zirconium oxides, which influences the optimal conditions of the traveling-solvent floating-zone (TSFZ) crystal growth. Adding the fact that crystals were grown at various institutions using different equipment, the result is that single-crystal samples of $Pr_2Zr_2O_7$ and $Pr_2Hf_2O_7$ have proved different in their level of structural disorder. Given the potential influence of disorder around non-Kramers ions [30], a short summary can be that the results of previous studies on $Pr_2Zr_2O_7$ differ from our work on $Pr_2Hf_2O_7$ in the extent to which samples reflect disorder in the physics of the system. In particular, it seems likely that strong disorder in samples of $Pr_2Zr_2O_7$ leads to degrees of freedom having essentially a quadrupolar character [48-50] (although other scenarios have been proposed [51]), while the reduced level of disorder in $Pr_2Hf_2O_7$ preserves magnetic dipoles and introduces quantum fluctuations on the spin ice manifold [18]. A clear experimental signature of this difference is that spin ice-like scattering is found in the quasi-elastic channels in $Pr_2Hf_2O_7$ [18] – as expected from a QSI, while all studies on $Pr_2Zr_2O_7$ have essentially shown signals centered on finite energy transfers around 0.3 meV [48-49,51-53].

It should be noted here that the quasi-elastic map published in the first study of $Pr_2Zr_2O_7$, by Kimura et al. [52], interpreted this signal as evidence for short-range spin ice correlations static on the scale of 2 picoseconds – corresponding to the finite energy-resolution of their experiment. Such a resolution (equivalently 0.38 meV) thus integrates over a range including the energy scale of the interactions in Pr-based pyrochlores, where inelastic scattering can be expected. This isn't an issue for the $Pr_2Zr_2O_7$ data as it was found that there is essentially no quasi-elastic contribution in the studied samples [48-49,51-53]. However, it is worth making this point when comparing with $Pr_2Hf_2O_7$, where the resolution of our measurements on IN5 (0.050 meV) is crucial for a clean separation of quasi-elastic and inelastic scattering [18]. It turns out that a quasi-elastic signal of the type expected in a QSI is measurable in $Pr_2Hf_2O_7$, and that its q-dependence is distinguishable from the "starfish" scattering observed at finite energy transfers and ascribed to the gapped excitations of the QSI state.

Finally, we should certainly mention here the recent interest on Ce^{3+}-based pyrochlores. On the basis of bulk measurements and muon spin relaxation experiments, $Ce_2Sn_2O_7$ was identified as a candidate material for the realization of a quantum spin liquid state on the pyrochlore lattice [54]. It was then pointed by theoreticians that the bulk properties support the existence of a 'dipole-octupole' ground state doublet [55], meaning that the degrees of freedom are magnetic octupoles in directions perpendicular to the local trigonal direction of the magnetic dipoles. Recently, neutron scattering experiments were reported on the related zirconate compound

[56-57]. Though being at an early stage, these results further confirm the interest of Ce^{3+}-based pyrochlores.

CONCLUSIONS AND OUTLOOK

Our neutron scattering study of $Pr_2Hf_2O_7$ reveals signatures of a quantum spin ice ground state. Such observations constitute a concrete example of a three-dimensional quantum spin liquid – a topical state of matter that has so far mostly been observed in lower dimensions. First, the mapping of the quasi-elastic structure factor at 0.05 K in this material reveals pinch points (Figures 2 and 3) – a signature of a classical spin ice – that are partially suppressed, as expected in a quantum spin ice. The line shape of the pinch-point scattering was compared with calculations of a lattice field theory of a quantum spin ice, in which low-energy gapless photon excitations explain the broadening of the curve. This result allows an estimate for the speed of light associated with magnetic photon excitations. Second, our data also reveal a continuum of inelastic spin excitations (Figure 4), which resemble predictions for the fractionalized, topological excitations of a quantum spin ice. Taken together, these two signatures strongly suggest that the low-energy physics of $Pr_2Hf_2O_7$ can be described by emergent quantum electrodynamics.

Further experimental work is needed to fully characterize the low temperature state of $Pr_2Hf_2O_7$. This includes careful measurements of the heat capacity down to very low temperature in order to compare its temperature dependence with predictions for linearly-dispersing photons, and to determine the entropy associated with the spin-liquid state. Moreover, detailed predictions of how pinch points evolve with temperature exist and such measurements would provide important information about quantum coherence in the QSI state. Finally, directly probing the photons through higher resolution techniques, using for example neutron spin echo or back-scattering instruments, is one of the ultimate experimental goals in a QSI material.

REFERENCES

[1] Pauling, L. *J. Am. Chem*. Soc. **57**, 2680 (1935).
[2] Castelnovo, C., Moessner, R. & Sondhi, S. L. *Annu. Rev. Condens. Matter Phys.* **3**, 35–55 (2012).
[3] Balents, L. Nature **464**, 199–208 (2010).
[4] Savary, L & Balents, L. *Rep. Prog. Phys.* **80**, 016502 (2016).
[5] Anderson, P. W. *Mat. Res. Bull.* **8**, 153 (1973).
[6] Tennant, D. A., Perring, T. G., Cowley, R. A., & Nagler, S. E. *Phys. Rev. Lett,* **70** 4003–4006 (1993).
[7] Han, T.-H. *et al. Nature* **492**, 406–410 (2012).
[8] Banerjee, A. *et al. Nature Mater.* **15**, 733–740 (2016).
[9] Shen, Y. *et al. Nature* **540**, 559–562 (2016).
[10] Gingras, M. J. P. and McClarty, P. A., *Rep. Prog. Phys.* **77**, 056501 (2014).

[11] Henley, C. L. *Annu. Rev. Condens. Matter Phys.* **1**, 179-210 (2010).
[12] Castelnovo, C., Moessner, R. & Sondhi, S. L. *Nature* **451**, 42–45 (2008).
[13] Hermele, M., Fisher, M. P. A. & Balents, L. *Phys. Rev. B* **69**, 064404 (2004).
[14] Rau, J. G. and Gingras, M. J. P., *Ann. Rev. Condens. Matter 10.1146/annurev-conmatphys-022317-110520* (2018).
[15] Petit, S., Lhotel, E. *et al.*, Nature Phys. **12**, 146-750 (2016).
[16] Lhotel, E., Petit, S. *et al.*, Nature Commun. **9**, (2018) 3786 (2018).
[17] Fennell, T. *et al. Science* **326**, 415 (2009).
[18] Sibille, R. *et al. Nature Physics* **14**, 711-715 (2018).
[19] Sibille, R. *et al. Phys. Rev. B* **94**, 024436 (2016).
[20] Shannon, N., Sikora, O., Pollmann, Penc, K. & Fulde, P. *Phys. Rev. Lett.* **108**, 067204 (2012).
[21] Benton, O., Sikora, O. & Shannon, N. *Phys. Rev. B* **86**, 075154 (2012).
[22] Wan, Y., Carrasquilla, J. & Melko, R. G. *Phys. Rev. Lett.* **116**, 167202 (2016).
[23] Hao, Z., Day, A. G. R. & Gingras, M. J. P. *Phys. Rev. B* **90**, 214430 (2014).
[24] Petrova, O., Moessner, R. & Sondhi, S. L. *Phys. Rev. B* **92**, 100401(R) (2015).
[25] Udagawa, M. and Moessner R. *Phys. Rev. Lett.* **122**, 117201 (2019).
[26] Kato, S. & Onoda, S. *Phys. Rev. Lett.* **115**, 077202 (2015).
[27] Curnoe, S. H. *Phys. Rev. B* **78**, 094418 (2008).
[28] Ross, K. A., Savary, L., Gaulin, B. D. & Balents, L. *Phys. Rev. X* **1**, 021002 (2011).
[29] Onoda, S. & Tanaka, Y. *Phys. Rev. Lett.* **105**, 047201 (2010).
[30] Savary, L. and Balents, L. *Phys. Rev. Lett.* **118**, 087203 (2017).
[31] Benton, O. *Phys. Rev. Lett.* **121**, 037203 (2018).
[32] Ciomaga-Hatnean, M. *et al. J. Phys.: Condens. Matter* **29**, 075902 (2017).
[33] Chen, G. *Phys. Rev. B* **96**, 195127 (2017).
[34] Champion, J. D. M. *et al. Phys. Rev. B* **68**, 020401 (2003).
[35] Savary, L., Ross, K. A., Gaulin, B. D., Ruff, J. P. C. and Balents, L. *Phys. Rev. Lett.* **109**, 167201 (2012).
[36] Yan, H., Benton, O., Jaubert, L. and Shannon, N. *Phys. Rev. B* **95**, 094422 (2017).
[37] Robert, J. *et al. Phys. Rev. B* **92**, 064425 (2015).
[38] Jaubert, L. D. C. *et al. Phys. Rev. Lett.* **115**, 267208 (2015).
[39] Benton, O. *Phys. Rev. B* **94**, 104430 (2016).
[40] Fennell, T., Kenzelmann, M., Roessli, B., Haas, M. K. and Cava, R. J. *Phys. Rev. Lett.* **109**, 017201 (2012).
[41] Guitteny, S. *et al. Phys. Rev. Lett.* **111**, 087201 (2013).
[42] Fennell, T. *et al. Phys. Rev. Lett.* **112**, 017203 (2014).
[43] Constable, E. *et al. Phys. Rev. B* **95**, 020415(R) (2017).
[44] Takatsu, H. *et al. Phys. Rev. Lett.* **116**, 217201 (2016).
[45] Kadowaki H. *et al. J. Phys. Soc. Jpn.* **87,** 064704 (2018).
[46] Kadowaki H. *et al. Phys. Rev. B* **99**, 014406 (2019).
[47] Molavian, H. R., Gingras, M. J. P. and Canals, B. *Phys. Rev. Lett.* **98**, 157204 (2007).
[48] Petit, S, Lhotel, E. *et al. Phys. Rev. B* **94**, 165153 (2016).
[49] N. Martin *et al. Phys. Rev. X* **7**, 041028 (2017).
[50] Benton, O. *Phys. Rev. Lett.* **121**, 037203 (2018).
[51] Wen, J.-J. *et al. Phys. Rev. Lett.* **118**, 107206 (2017).
[52] Kimura, K. *et al. Nat Commun* **4**:1934 (2013).
[53] Alannah Hallas, $Ho_2Ge_2O_7$ and $Pr_2Zr_2O_7$: A Tale of Two Spin Ices, Master's thesis, Department of Chemistry, University of Manitoba (2013).
[54] Sibille, R. *et al. Phys. Rev. Lett.* **115**, 097202 (2015).
[55] Li, Y-D. and Chen, G. *Phys. Rev. B* **95**, 041106(R) (2017).
[56] Gao, B. *et al. arXiv:1901:10092*.
[57] Gaudet, J. et al. arXiv:1903:09207.

Spin Correlations in Frustrated Spinels

Shang Gao,[1,2,3,*] Oksana Zaharko,[1] Tom Fennell,[1] Vladimir Tsurkan,[4,5] and Christian Rüegg[1,2]
[1]Laboratory for Neutron Scattering and Imaging, Paul Scherrer Institut, CH-5232 Villigen PSI, Switzerland
[2]Department of Quantum Matter Physics, University of Geneva, CH-1211 Geneva, Switzerland
[3]RIKEN Center for Emergent Matter Sciences, JP-3510106 Wako, Japan
[4]Experimental Physics V, University of Augsburg, D-86135 Augsburg, Germany
[5]Institute of Applied Physics, Academy of Sciences of Moldova, MD-2028 Chisinau, Republic of Moldova

(Dated: January 21, 2019)

Abstract

Spinels of the chemical formula AB_2X_4 are important systems in the study of frustrated magnetism. Their A and B sites constitute the diamond and pyrochlore lattices, respectively, whose special geometries might lead to exotic spin correlations. In this article, we discuss our neutron scattering works on the frustrated spinels. We focus on two representative systems: $CdEr_2X_4$ (X = Se, S) where the B-site Er^{3+} spins manifest the spin ice correlations and $MnSc_2S_4$ where the A-site Mn^{2+} spins give rise to the spiral spin-liquid state.

INTRODUCTION TO FRUSTRATED MAGNETISM

The main idea of introducing frustration to magnetic systems is to enhance quantum and thermal fluctuations. In this way, the classical ground state is no longer that favored and the resulting state might be quite exotic [1]. An illustrating example can be found in Fig. 1, where we compare the ground state energy of two antiferromagnetically-coupled spin plaquettes. For the un-frustrated square plaquette, all the four nearest-neighbour pairs are anti-parallel and the ground state energy is $-|J|S^2$ per spin. While for the frustrated tri-

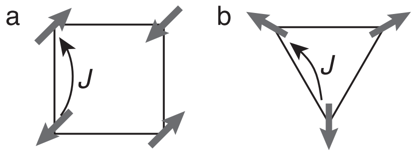

Fig. 1
Classical ground state configurations for nearest-neighbour antiferromagnetically coupled square (a) and triangular (b) plaquette.

angular plaquette, the neighbouring spins define a 120° angle and the ground state energy becomes $-|J|S^2/2$ per spin, which is much higher than the unfrustrated case. Therefore, the classical long-range ordered states for frustrated lattices become less favorable in energy, leaving more 'room' for thermal and quantum fluctuations to play a role. One well-known example is the resonating-valence-bond state initially proposed by Fazekas and Anderson [2], where the classical long-range order is completely removed by quantum fluctuations and the low energy excitations are S=1/2 spinons rather than the conventional S=1 magnons.

One important consequence of frustration is the huge degeneracy of the ground states, and this is especially true for the classical systems with relatively large spins. We may take the kagomé lattice as an example, which is constituted of corner-sharing triangles. Assuming an equal antiferromagnetic coupling strength for all the nearest-neighbour bonds, the spin Hamiltonian $\mathcal{H} = J\sum_{\langle ij\rangle} S_i S_j$, where i,j denote different spin sites, can be transformed to $\mathcal{H} = 1/2J\sum_{\Delta}(S_{\Delta})^2$ + const, where Δ indexes different triangles and S_{Δ} is the sum of the total spin over the triangle Δ. It is immediately clear that any state with zero total moment over the triangles can be the ground state.

On the other hand, we know that most of the classical systems will finally settle into a unique long-range ordered state at low temperature. Then how this ground-state degeneracy is relieved becomes an interesting question. Several perturbations might play a role. One is further neighbor couplings, which add more constraints to the ground state manifold. Another possibility is spin-lattice coupling. This works because the super-exchange interaction usually depends on the distance between the spins. If there is a lattice distortion, the strength of exchange couplings will become different, so that the degeneracy of the ground state might be relieved. Finally, even the thermal fluctuations might relieve the ground state degeneracy. The reason is that although the ground states have equal

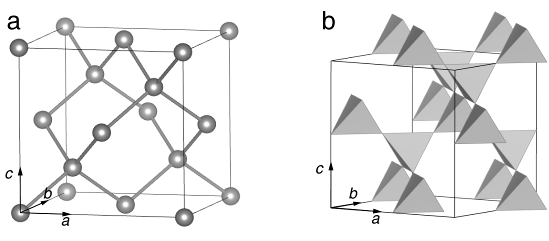

Fig. 2
The diamond (a) and pyrochlore (b) lattice formed by the A and B sites of the spinel, respectively.

energies, their low energy excitations might be very different. If there is some state that is extremely prone to low energy excitations, it might be favored by thermal fluctuations as the long-range ordered state, leading to the order-by-disorder transition.

In this article, we concentrate on the spinel systems AB_2X_4, where the A and B sites constitute diamond and pyrochlore lattices, respectively (see Fig. 2). With our neutron scattering works on $CdEr_2X_4$ (X = Se, S) and $MnSc_2S_4$, we are able to observe how different lattice geometries are influencing the spin behavior and give rise to rich correlated states [3, 4].

SPIN ICE STATES IN $CdEr_2X_4$

In the water ice, there are four O-H bonds around each oxygen ions: two are short covalent bonds and two are long hydrogen bonds, which leads to the 2-near-2-far ice-rule of the hydrogen position. A similar state can be realized on the pyrochlore lattice, where the spins on the vertex of the tetrahedra obey a 2-in-2-out ice-rule [5, 6]. To realize such a spin ice state, two conditions must be satisfied. Firstly, the spins should be constrained by the local crystal electric field (CEF) to the lines that connect the centers of the tetrahedra; Secondly, the coupling between the spins should be ferromagnetic so that the 2-in-2-out state is the ground state. The existence of the spin ice state has been well established in the pyrochlore titanates like $Dy_2Ti_2O_7$ and $Ho_2Ti_2O_7$, where the nearest-neighbour couplings are dominated by ferromagnetic dipolar interactions [5, 6].

Recent transport measurements revealed the spinel compound of $CdEr_2Se_4$ to be the first spin ice candidate beyond the pyrochlores and calls for neutron scattering studies to provide the microscopic evidence [7]. Follow-

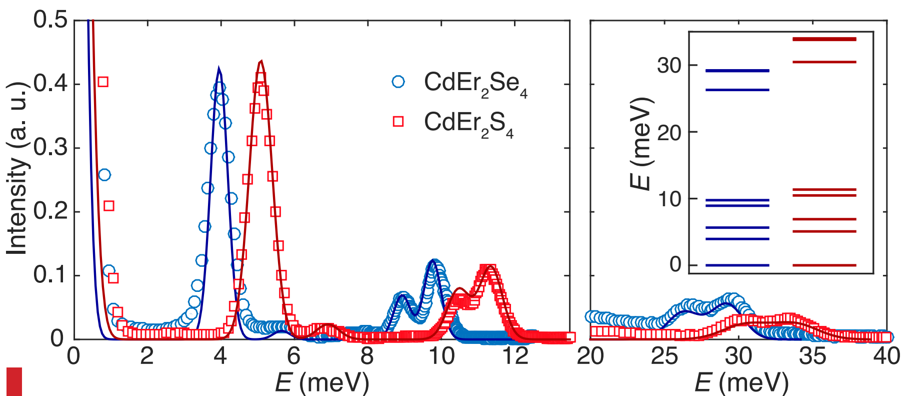

Fig. 3
(color online). Inelastic neutron scattering results of the CEF transitions in $CdEr_2Se_4$ (measured at T = 2 K) and $CdEr_2S_4$ (measured at T = 1.5 K). Error bars are smaller than the symbol size. The fits are shown as solid lines. The inset shows the fitted energies of the CEF levels for $CdEr_2Se_4$ (left column) and $CdEr_2S_4$ (right column).

	B_2^0	B_4^0	B_4^3	B_6^0	B_6^3	B_6^6
$CdEr_2Se_4$	-25.70	-107.73	-97.74	25.31	-19.06	9.51
$CdEr_2S_4$	-29.18	-122.72	-113.66	25.97	-21.89	14.41
J_z	$\pm 15/2$	$\pm 9/2$	$\pm 3/2$	$\mp 3/2$	$\mp 9/2$	
$CdEr_2Se_4$	± 0.906	0.386	± 0.159	-0.073	± 0.004	
$CdEr_2S_4$	± 0.904	0.391	± 0.145	-0.094	± 0.006	

Table 1
The fitted Wybourne CEF parameters (meV) and ground state doublets for $CdEr_2Se_4$ and $CdEr_2S_4$.

ing the two conditions discussed previously, we first employ inelastic neutron scattering to prove the Ising character of the Er^{+3} spins in $CdEr_2Se_4$ and $CdEr_2S_4$, and then use diffuse neutron scattering to prove the ferromagnetic character of the spin interactions.

Our powder samples of $CdEr_2Se_4$ and $CdEr_2S_4$ were synthesized by the solid-state reaction method. To reduce neutron absorption, the ^{114}Cd isotope was used. Fig. 3 presents the inelastic neutron scattering results of the CEF transitions in $CdEr_2Se_4$ and $CdEr_2S_4$ collected on IN4 at Institut Laue-Langevin (ILL) with 1.21 and 2.41 Å incident neutron wavelengths. Altogether 6 peaks are observed at the base temperature for both compounds, which is consistent with the Stokes transitions within the Er^{3+} $^4I_{15/2}$ manifold under D_{3d} symmetry. Using the McPhase program [8], we fitted the measured spectra with the CEF Hamiltonian $H = \sum_{lm} B_l^m \hat{O}_l^m$, where $\hat{O}_l^m$ are the Stevens operators and B_l^m are the corresponding coefficients. The fitting results are shown in Fig. 3 as the solid lines and Table I lists the fitted CEF parameters and ground state wavefunctions. Specifically, the wavefunctions for both of the ground state doublets are dominated by the $|15/2, \pm 15/2\rangle$ components and have almost the same anisotropic g-factors of $g_\perp = 0$ and $g_\parallel = 16.4$, which is consistent with the previous report for $CdEr_2Se_4$ [7]. Thus our inelastic neutron scattering results confirm the Ising character of the Er^{3+} spins in $CdEr_2Se_4$ and $CdEr_2S_4$.

Next, we used diffuse neutron scattering to study the short spin correlations. Fig. 4 presents the quasi-static spin-spin correlations in $CdEr_2Se_4$ obtained from polarized neutron diffuse scattering. The experiment was performed on D7 at ILL with a 4.8 Å setup [9].

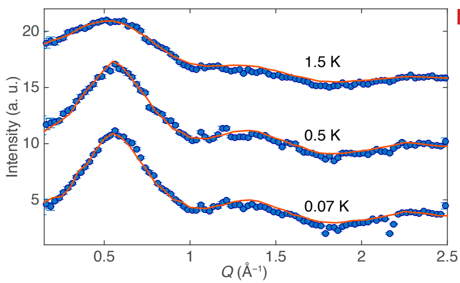

Fig. 4
(color online). $CdEr_2Se_4$ magnetic scattering at 0.07, 0.5, and 1.5 K obtained from the xyz polarization analysis. The 0.5 (1.5) K data is shifted by 6 (12) along the y axis. The Monte Carlo simulation results are shown as solid red lines.

Broad peaks are observed at 0.6 and 1.4 Å −1, and the overall pattern is very similar to that of the known dipolar spin ices [10–12].

To fit the observed spin-spin correlations in $CdEr_2Se_4$, we performed single-spin-flip Monte Carlo simulations for the dipolar spin ice model with exchange couplings up to the second neighbors [13]:

$$\mathcal{H} = J_1 \sum_{\langle ij \rangle} \sigma_i \sigma_j + J_2 \sum_{\langle\langle ij \rangle\rangle} \sigma_i \sigma_j + D r_0^3 \sum_{ij} \left[\frac{\vec{n}_i \cdot \vec{n}_j}{|r_{ij}|^3} - \frac{3(\vec{n}_i \cdot \vec{r}_{ij})(\vec{n}_j \cdot \vec{r}_{ij})}{|r_{ij}|^5} \right] \sigma_i \sigma_j. \quad (1)$$

Here, $\vec{n}_i$ is the unit vector along the local ⟨111⟩ axes with the positive direction pointing from one diamond sublattice of the tetrahedra center to the other, $\sigma_i = \pm 1$ is the corresponding Ising variable, J_1 and J_2 are the exchange interactions for first-neighbors (NN) ⟨ij⟩ and second-neighbors ⟨⟨ij⟩⟩, respectively, r_0 is the NN distance, and D is the dipolar interaction, 0.616 and 0.690 K for $CdEr_2Se_4$ and $CdEr_2S_4$, respectively. With the ALPS package [14], we implemented the Hamiltonian (1) on a 6 × 6 × 6 supercell with periodic boundary conditions. Assuming the effective NN coupling $J_{eff} = J_1 + 5D/3$ to be equal to 1 K at which temperature the $CdEr_2Se_4$ specific heat maximum was observed [7], we fixed J_1 to −0.027 K and only varied J_2 in the fitting process. As is shown in Fig. 4, the model with J_2 = 0.042 K fits the measured spin correlations very well. Therefore, our simulations confirm the dominance of the dipolar interactions in $CdEr_2Se_4$. Non-polarized neutron diffuse scattering results for $CdEr_2S_4$ have similar Q-dependence as that of $CdEr_2Se_4$ and can be fitted by the dipolar spin ice model as well. In this way, we establish the existence of the dipolar spin ice state in $CdEr_2Se_4$ and $CdEr_2S_4$.

SPIRAL SPIN-LIQUID AND THE EMERGENCE OF A TRIPLE-Q VORTEX-LIKE STATE IN $MnSc_2S_4$

The A sites of the spinel AB_2X_4 constitute a diamond lattice and its frustration mainly comes from the competition between the first-neighbour coupling J_1 and second-neighbour coupling J_2 [15]. Starting from the J_1-J_2 Hamiltonian [15]:

$$\mathcal{H} = J_1 \sum_{\langle ij \rangle} S_i \cdot S_j + J_2 \sum_{\langle\langle ij \rangle\rangle} S_i \cdot S_j, \quad (2)$$

it is found that when $|J_2/J_1| > 1/8$, the propagation vector **q** of the ground state forms a two-dimensional surface in reciprocal space. Fig. 5 plots the spiral surface for the case of $|J_2/J_1| = 0.85$. Since each **q** position over this surface represents a spiral state, such a surface is called the 'spiral surface'. Furthermore,

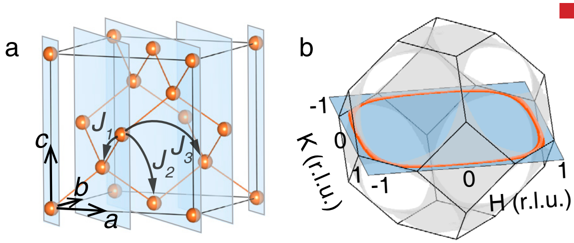

Fig. 5
Diamond lattice of Mn^{2+} ions in $MnSc_2S_4$, (110) planes are shaded blue. (b) Spiral surface (gray) predicted by mean-field theory for the J_1-J_2 model with the ratio $|J_2/J_1|$ = 0.85. The red ring emphasizes a cut within the (HK0) plane (blue). (c).

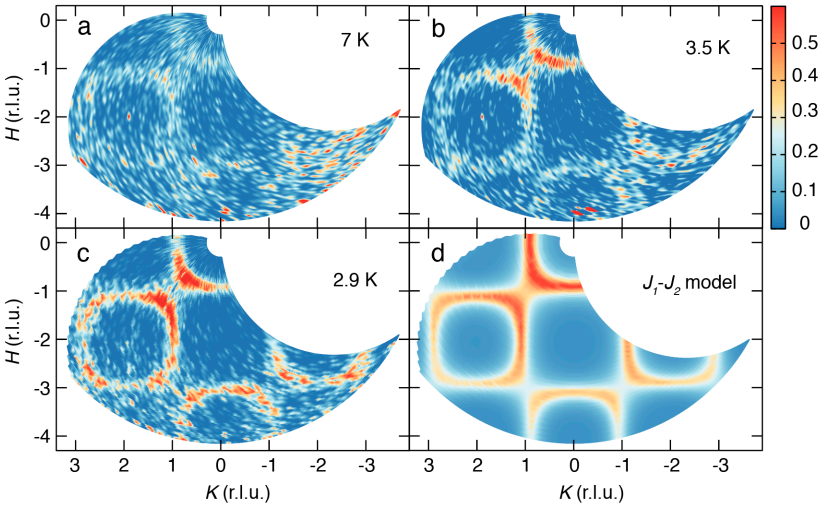

Fig. 6

Magnetic diffuse scattering in the (hk0) plane of $MnSc_2S_4$ measured at T = 2.9 **(a)**, 3.5 **(b)**, and 7 K **(c)**. A measurement at 50 K has been subtracted as the background. Panel d shows the Monte Carlo simulation results using the J_1-J_2 model with the ratio $|J_2/J_1| = 0.85$ and $T/|J_1| = 0.55$.

when all the possible spiral states are populated at the same time, the system then realizes the so-called spiral spin-liquid state [15].

Although $MnSc_2S_4$ has been viewed as a promising candidate to realize the spiral spin-liquid state [15, 16], there have been no direct observation of the spiral surface due to the lack of single crystal sample. Recently we managed to grow high quality $MnSc_2S_4$ single crystals and the direct exploration of the spin correlations in reciprocal space becomes possible.

Fig. 6a-c presents our magnetic diffuse scattering results at T = 7.0, 3.5, and 2.9 K obtained on DNS at Heinz Maier-Leibnitz Zentrum (MLZ) using polarized neutron with an incoming wavelength of 4.5 Å. With decreasing temperature, a squared-ring pattern gradually appear, which evidences the existence of the spiral surface. In order to fix the ratio J_2/J_1, Monte Carlo simulations were performed. As is compared in Fig. 6, the simulation with $|J_2/J_1| = 0.85$ and $T/|J_1| = 0.55$ can reproduce the experimental data very well. This high value of $|J_2/J_1|$ puts $MnSc_2S_4$ deep in the spiral spin-liquid phase and establishes it as the first A-site spinel that realizes the spiral spin-liquid state.

Besides the spiral spin-liquid state, we also investigated the long-range ordered state at $T < T_N$. For that purpose, we performed single crystal neutron diffraction experiments on TriCS at the Swiss Spallation Neutron Source (SINQ) of Paul Scherrer Institut (PSI) and also spherical neutron polarimetry experiments on TASP with MuPAD at SINQ and IN22 with CryoPAD at ILL. Our experiments reveal multiple transitions: at 2.2 K, the system first enters a sinusoidally modulated collinear phase with **q** = (0.75 0.75 0); at 1.64 K, it then

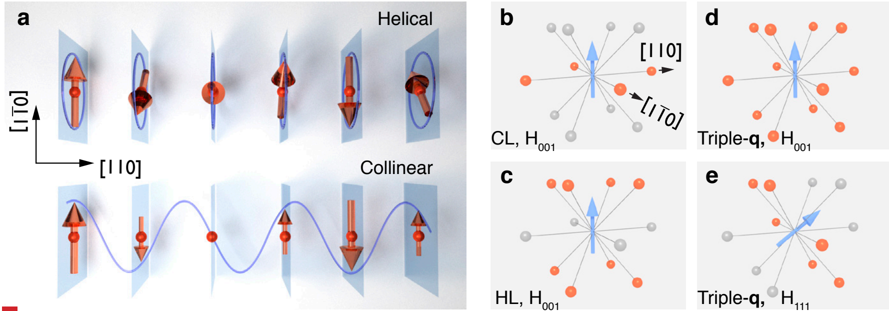

Fig. 7
Comparison between the observed and calculated intensities of the **(a)** helical and **(b)** collinear phases. **(c)** The helical structure (top) and the sinusoidally-modulated collinear structure (bottom) refined from the data at 1.38 and 1.70 K. Blue shaded planes are perpendicular to the propagation vector (e.g., (110) planes for $\mathbf{q}$ = (0.75 0.75 0), which are also shown in the crystal structure of Fig. 5); In these planes the ordered moments have the same size and orientation.

enters a transitional incommensurate phase with $\mathbf{q}$ = (0.75 ± 0.02 0.75 ∓ 0.02 0); and finally, at 1.46 K, the system enters a helical phase with $\mathbf{q}$ back to the (0.75 0.75 0) position. Such a multi-step transition is a direct evidence for the importance of perturbations from the thrid-neighbour coupling J_3 and the dipolar interactions.

The established collinear and helical phases are both single-$\mathbf{q}$ structures, meaning that the 12 arms of the ⟨0.75 0.75 0⟩ star form independent magnetic domains. Fig. 7b,c summarize the response of all the 12 arms for the collinear and helical phases when we applied a magnetic field along the [001] direction. However, after cooling from the collinear phase in a field of 3.5 T, refinements of the neutron diffraction datasets reveal that although the single-arm structure stays the same, the previously suppressed arms re-appear with all the 12 arms having about the same intensities. This intensity re-distribution, which is summarized in Fig. 7e, is contradictory to the domain effect expected for a single-$\mathbf{q}$ structure, and evidences the emergence of a field-induced multi-$\mathbf{q}$ phase. By studying the H and T dependence of the intensity of the (0.75 0.75 0) Bragg peak, the extent of this multi-$\mathbf{q}$ phase is mapped out in Fig. 8.

We propose the field-induced phase to be a triple-$\mathbf{q}$ state with:

$$\mathbf{M}(\mathbf{r}) = \sum_{j=1}^{3}(\mathbf{m}_j e^{i(\mathbf{q}_j\cdot\mathbf{r}+\phi_j)} + \mathrm{c.\,c.}), \qquad (3)$$

where the three coplanar $\mathbf{q}_j$ satisfy $\sum_{j=1}^{3}\mathbf{q}_j = 0$ (*e.g.*, $\mathbf{q}_1 = (0.75\ 0.75\ 0)$, $\mathbf{q}_2 = (0\ \overline{0.75}\ 0.75)$, and $\mathbf{q}_3 = (\overline{0.75}\ 0\ \overline{0.75})$), similar to that observed in the skyrmion lattice [17]; m_j is the real basis vector perpendicular to q_j; φ_j describes an additional phase factor; and c.c. is the complex conjugate. Four triple-$\mathbf{q}$ domains formed in this way are symmetrically equivalent under the [001] magnetic field, which explains the equal intensity distribution shown in Fig. 7d. In contrast, in Fig. 7e we plot the distribution measured under a 3.5 T magnetic field along the [111] direction. This [111] field breaks the symmetry and therefore only one triple-**q** domain with arms perpendicular to H can be observed.

Although neutron diffraction is not sensitive to the phase factor φ_j and the triple-**q** structure cannot be uniquely defined, we find that no matter what specific values of φ_j are chosen, there is always a winding feature in the generated magnetic structure. Therefore, this triple-**q** phase in $MnSc_2S_4$ actually realizes the vortex state recently predicted in frustrated antiferromagnets [18].

CONCLUSION

Using neutron scattering, we have investigated the spin correlations in two representative spinel systems of $CdEr_2X_4$ (X = S, Se) and $MnSc_2S_4$. Due to the special geometry of the diamond lattice of the A sites and the pyrochlore lattice of the B sites, very unusual spin correlations have been revealed: the Er^{3+} spins in $CdEr_2X_4$ are found to mimic the behavior of water ice; while the Mn^{2+} spins form a spiral spin-liquid state and give rise to a triple-**q** state under magnetic field.

ACKNOWLEDGEMENTS

This contribution summarizes part of the PhD thesis [19] and published manuscripts [3, 4] of Shang Gao. It is based on neutron scattering experiments performed at the Swiss Spallation Neutron Source SINQ, Paul Scherrer Institut, Villigen, Switzerland, the Heinz Maier-Leibnitz Zentrum MLZ, Garching, Germany, and the Institut Laue-Langevin ILL, Grenoble, France. This work was supported by the Swiss National Science Foundation under Grants No. 20021-140862, No. 20020-152734, and the SCOPES project No. IZ73Z0- 152734/1.

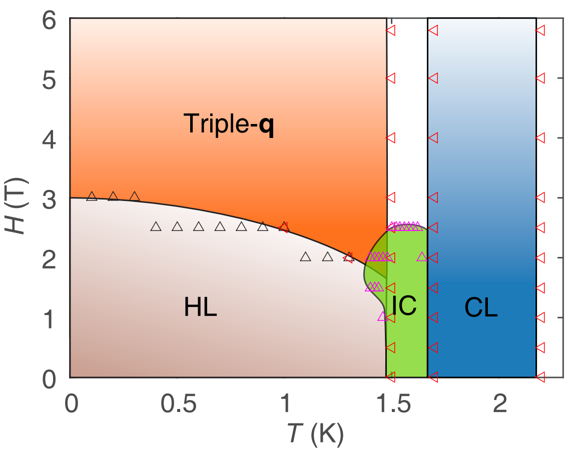

Fig. 8
Phase diagram from neutron diffraction experiments. Up-pointing (left-pointing) triangles mark the transition positions extracted from the measurements with increasing field (decreasing temperature). HL, CL and IC represent the helical, sinusoidally-modulated collinear, and incom- mensurate phases, respectively. The IC phase disappears under field cooling.

* shang.gao@riken.jp

[1] Claudine Lacroix, Philippe Mendels, and Frédéric Mila, *Introduction to Frustrated Magnetism* (2010).

[2] P. Fazekas and P. W. Anderson, "On the ground state properties of the anisotropic triangular antiferromagnet," Philos. Mag. **30**, 423–440 (1974).

[3] Shang Gao, Oksana Zaharko, Vladimir Tsurkan, Yixi Su, Jonathan S. White, Gregory S. Tucker, Bertrand Roessli, Frederic Bourdarot, Romain Sibille, Dmitry Chernyshov, Tom Fennell, Alois Loidl, and Christian Rüegg, "Spiral spin-liquid and the emergence of a vortex-like state in $MnSc_2S_4$," Nature Physics **13**, 157 (2017).

[4] Shang Gao, O. Zaharko, V. Tsurkan, L. Prodan, E. Riordan, J. Lago, B. Fåk, A. R. Wildes, M. M. Koza, C. Ritter, P. Fouquet, L. Keller, E. Canévet, M. Medarde, J. Blomgren, C. Johansson, S. R. Giblin, S. Vrtnik, J. Luzar, A. Loidl, Ch. Rüegg, and T. Fennell, "Dipolar spin ice states with a fast monopole hopping rate in $CdEr_2X_4$ (X = S, Se)," Phys. Rev. Lett. **120**, 137201 (2018).

[5] Steven T Bramwell and Michel J P Gingras, "Spin ice state in frustrated magnetic pyrochlore materials," Science **294**, 1495–1501 (2001).

[6] T Fennell, P P Deen, A R Wildes, K Schmalzl, D Prabhakaran, A T Boothroyd, R J Aldus, D F McMorrow, and S T Bramwell, "Magnetic coulomb phase in the spin ice $Ho_2Ti_2O_7$," Science **326**, 415–417 (2009).

[7] J Lago, I Živković, B Z Malkin, J Rodriguez Fernandez, P Ghigna, P Dalmas de Réotier, A Yaouanc, and T Rojo, "$CdEr_2Se_4$: A new erbium spin ice system in a spinel structure," Phys. Rev. Lett. **104**, 247203 (2010).

[8] M. Rotter, "Using mcphase to calculate magnetic phase diagrams of rare earth compounds," J. Mag. Magn. Mater. **272-276,** E481–E482 (2004).

[9] G. Ehlers, J. R. Stewart, A. R. Wildes, P. P. Deen, and K. H. Andersen, "Generalization of the classical xyz-polarization analysis technique to out-of-plane and inelastic scattering," Rev. Sci. Instr. **84**, 093901 (2013).

[10] H. Kadowaki, Y. Ishii, K. Matsuhira, and Y. Hinatsu, "Neutron scattering study of dipolar spin ice $Ho_2Sn_2O_7$: frustrated pyrochlore magnet," Phys. Rev. B **65**, 144421 (2002).

[11] Isabelle Mirebeau and Igor Goncharenko, "Spin liquid and spin ice under high pressure: a neutron study of $R_2Ti_2O_7$ (R = Tb,Ho)," Journal of Physics: Condensed Matter **16**, S653 (2004).

[12] A. M. Hallas, J. A. M. Paddison, H. J. Silverstein, A. L. Goodwin, J. R. Stewart, A. R. Wildes, J. G. Cheng, J. S. Zhou, J. B. Goodenough, E. S. Choi, G. Ehlers, J. S. Gardner, C. R. Wiebe, and H. D. Zhou, "Statics and dynamics of the highly correlated spin ice $Ho_2Ge_2O_7$," Phys. Rev. B **86**, 134431 (2012).

[13] Taras Yavors'kii, Tom Fennell, Michel J P Gingras, and Steven T Bramwell, "$Dy_2Ti_2O_7$ spin ice: A test case for emergent clusters in a frustrated magnet," Phys. Rev. Lett. **101**, 037204 (2008).

[14] B. Bauer, L. D. Carr, H. G. Evertz, A. Feiguin, J. Freire, S. Fuchs, L. Gamper, J. Gukelberger, E. Gull, S. Guertler, A. Hehn, R. Igarashi, S. V. Isakov, D. Koop, P. N. Ma, P. Mates, H. Matsuo, O. Parcollet, G. Pawłowski, J. D. Picon, L. Pollet, E. Santos, V. W. Scarola, U. Schollwöck, C. Silva, B. Surer, S. Todo, S. Trebst, M. Troyer, M. L. Wall, P. Werner, and S. Wessel, "The ALPS project release 2.0: open source software for strongly correlated systems," J. Stat. Mech.: Theo. and Exp. **2011**, P05001 (2011).

[15] Doron Bergman, Jason Alicea, Emanuel Gull, Simon Trebst, and Leon Balents, "Order-by-disorder and spiral spin-liquid in frustrated diamond-lattice antiferromagnets," Nat. Phys. **3**, 487–491 (2007).

[16] V. Fritsch, J. Hemberger, N. Büttgen, E. W. Scheidt, H. A. Krug von Nidda, A. Loidl, and V. Tsurkan, "Spin and orbital frustration in $MnSc_2S_4$ and $FeSc_2S_4$," Physical Review Letters **92**, 116401 (2004).

[17] S. Mühlbauer, B. Binz, F. Jonietz, C. Pfleiderer, A. Rosch, A. Neubauer, R. Georgii, and P. Böni, "Skyrmion lattice in a chiral magnet," Science **323**, 915–919 (2009).

[18] Tsuyoshi Okubo, Sungki Chung, and Hikaru Kawamura, "Multiple-q states and the skyrmion lattice of the triangular-lattice Heisenberg antiferromagnet under magnetic fields," Phys. Rev. Lett. **108**, 017206 (2012).

[19] Shang Gao, Doctoral Thesis: Neutron scattering investigation of the spin correlations in frustrated spinels (University of Geneva, 2017).

Announcements

The Name of the SGN/SNSS has changed to “Swiss Neutron Science Society”

The General Assembly of the Society on Nov. 26, 2018, has accepted to change the name of the Society from **“**Swiss Neutron Scattering Society**”** to the new name **“**Swiss Neutron Science Society**”**. This change of name reflects the openness of the society for all researchers who need access to neutron sources. See the Minutes of the General Assembly in this issue of Swiss Neutron News for more information.

SGN/SSDN Members

Presently the SGN/SSSN has 188 members. New members can register online on the SGN website: http://sgn.web.psi.ch

SGN/SSSN Annual Member Fee

The SGN/SSSN members are kindly asked to pay their annual member fees. At the general assembly 2013 of the society, the fee has been increased from CHF 10 to **CHF 20**. It can be paid either by bank transfer or in cash during your next visit at PSI. The bank account of the society is accessible for both Swiss national and international bank transfers:
Postfinance: 50-70723-6 (BIC: POFICHBE),
IBAN: CH39 0900 0000 5007 0723 6.

The SGN/SSSN is an organization with tax charitable status. All fees and donations payed to the SGN/SSSN are **tax deductible.**

PSI Facility News

Recent news and scientific highlights of the three major PSI user facilities SLS, SINQ and SμS can be found in the **quarterly electronic newsletter** available online under:
www.psi.ch/science/facility-newsletter

SINQ Upgrade

No neutrons are produced at the Swiss spallation neutron source SINQ in 2019, as SINQ receives a major upgrade in 2019 and 2020. The next call for beam-time proposals is planned to be launched early in 2020. Please visit the page:
www.psi.ch/sinq/call-for-proposals
to obtain the latest information.

Registration of publications

Please remember to **register all publications either based on data taken at SINQ, SLS, SμS or having a PSI co-author** to the Digital Object Repository at PSI (DORA):
www.dora.lib4ri.ch/psi/
Please follow the link 'Add Publication'.

Open Positions at SINQ and ILL

To look for open positions at SINQ or ILL, have a look at the following webpages:
www.psi.ch/pa/stellenangebote
www.ill.eu/careers/all-our-vacancies/?L=0

PhD positions at ILL

The PhD program of the Institut Laue-Langevin, ILL, is open to researchers in Switzerland. Consult the page www.ill.eu/science-technology/phd-students/home/
for information on the PhD program of ILL or get in contact with the managers of the program using the email address phd@ill.fr.
The Swiss agreement with the ILL includes that ILL funds and hosts one PhD student from Switzerland.

Minutes of the SGN/SSDN General Assembly 2018

Date/Location
November 26, 2018, Paul Scherrer Institut

Start
15:00

End
17:30

Participants
15 members of the society

1. Welcome

Henrik Ronnow, president of the Swiss Neutron Scattering Society, welcomes the participants to the general assembly 2018.

2. Minutes of the General Assembly 2017

The minutes of the general assembly of the SGN/SSDN from 3.11.2017, published in Swiss Neutron News #51 are accepted without objections.

3. Annual Report of the Chairman

H. Ronnow reports on the activities of the SGN/SSDN in the years 2017 and 2018:
a) The fourth (2017) and fifth (2018) Young Scientist Prize of the SGN/SSDN sponsored by Swiss Neutronics have been awarded to Dr. Viviane Lutz-Bueno and Dr. Shang Gao, respectively.
b) Two issues of Swiss Neutron News have appeared in April and October 2017 and another two have appeared in May and November 2018.
c) The SGN/SSDN has 212 members at the time of the assembly.

4. Report of the Treasurer

The annual balance sheet 2017 is presented:
Assets SGN/SSDN on 1.1.2017: **SFr 5789.35**

	Revenues [SFr]	**Expenses [SFr]**
Membership-fees (cash box)	60.00	
Membership-fees (postal check acc.)	340.00	
Donations	50.00	
Deposit prize money	1000.00	
Expenses Postfinance account		63.00
Payout prize money		1000.00
Total	1450.00	1063.00

Net earnings 2017	**SFr 387.00**	

Balance sheet 2017:	**Assets [SFr]**	**Liabilities [SFr]**
Postfinance account	4976.35	
Cash box	1200.00	
Assets on 31.12.2017	**6176.35**	

5. Report of the Auditors

Bericht der Revisoren

Die Rechnungsrevisoren haben die Belege, die Abrechnungen und die Bilanz für das Jahr 2017 geprüft und für in Ordnung befunden!

15.1.18 | M. Zolliker | 22.1.18 | Krämer
Datum | Dr. M. Zolliker, PSI | Datum | Dr. K. Krämer, Uni Bern

Both Auditors (K. Krämer and M. Zolliker) have examined the bookkeeping and the balance 2017. They have accepted it without objection.

The participants therefore unanimously vote for the release of the SGN/SSDN board.

6. Budget 2019

H. Ronnow presents the following proposal for the budget 2019:

	Receipts [SFr]	**Expenditures [SFr]**
member fees	500.00	
interest	0.00	
welcome reception		
fees PC account		63.00
Total	500.00	63.00
Total receipts 2019	437.00	
assets 31.12.2019	6613.35	

The participants accept the budget proposal unanimously. As in the general assembly 2017, the membership fees for students are discussed and it is again proposed that the membership for students could be free. A vote is taken, and free membership for students is accepted unanimously.

Christian Rüegg proposes that the SGN could sponsor an apéro at the SPS meeting linked to the session on neutron scattering to improve the visibility of the SGN.

Related to free membership for students, the bylaws of the SGN are discussed. There is a consensus that the bylaws should say clearly who has to pay membership fees and who has the right to take part in votes.

The idea of an on-line voting system is brought up, which would allow members to take part in votes without traveling to the general assembly. The board of SGN will prepare a proposal for clearer bylaws for the assembly in 2019, and a vote about any changes can be taken in 2019.

7.SGN board for the period 2019 – 2021

The term of the SGN board, Prof. Henrik Ronnow (president), Dr. Michel Kenzelmann, and PD Dr. Urs Gasser (secretary), ends in 2018. As announced at the general assembly in 2017,

H. Ronnow and U. Gasser are willing to stay on the SGN board for another term (2019–2021), while Prof. Michel Kenzelmann resigns. The board of SGN proposes Prof. Markus Strobl and PD Dr. Karl Krämer as new board members. Prof. Markus Strobl and PD Dr. Karl Krämer are elected without a dissentient vote. U. Gasser and H. Ronnow are unanimously re-elected as board member (secretary) and president of the society, respectively.

8. News from ENSA (H. Ronnow)

a. ENSA has participated as a partner in two proposals for EU funding for neutron sources in Europe. One of these, BrightnESS2, has been successful. ENSA will employ a coordinator for BrightnESS2.
b. Since 2015, Christiane Alba-Simionesco (LLB, France) is the chairperson of ENSA, and Ferenc Mezei (ESS) is the vice-chairman. Their term has ended but was extended until new chair persons are elected. The elections of the vice-chair have been started in autumn 2018, and the new vice-chair is expected to take over from Ferenc Mezei in spring 2019. The chair elections take place half a year later, and the new chair person will take over from Christiane Alba-Simionesco in autumn 2019. Nominations for the new chair can still be made.
c. H. Ronnow has been nominated for both the vice-chair and the chair of ENSA. If he is elected as the new chair of ENSA, SGN will have to find a new president. Other nominations for the chair are: Arantxa Arbe (Spain) and Laszlo Rosta (Hungary).

9. News from ILL (Ch. Rüegg)

a. The operation of ILL as a European neutron source has been extended until 2030. All member countries want to keep their membership for the next 5 years. Italy, however, has unresolved financial issues.
b. There have been uncertainties about the fuel for the ILL reactor, but fuel is now secured for the next 10 years.
c. The ILL has obtained 30 MEUR for new instrumentation to be realized in the MILLENNIUM and ENDURANCE programs.
d. The user operation in 2017 was interrupted due to cancelled beam cycles, which has caused a lot of backlog experiments for 2018. In 2018, all planned cycles took place and the postponed and new experiments could be completed.
e. The Swiss request for beam time in 2018 was again higher than the national balance for Switzerland. A few experiments were, therefore, shifted to the CRG instruments with Swiss participation.
f. From middle 2019 until middle 2020, ILL will have a long shutdown, which is used to install new beam tubes. This overlaps with the long shutdown of SINQ.

10. News from ESS (Ch. Rüegg)

a. First neutrons at ESS are planned for 2019. Delays in the construction, however, have pushed the commissioning of the first three instruments to 2023, this was previously planned for 2020/21. The user program is now planned to start in 2024, and ESS is planned to have 15 running instruments in 2029.

b. A smooth transition from the ILL to ESS and continuous access to a very intense neutron source is of great interest for Swiss neutron users. It will be the task of SGN to do the lobbying for this in Berne.
c. Switzerland is still involved in five instruments for ESS: ESTIA, BIFROST, HEIMDAL, ODIN and MAGIC. The reflectometer ESTIA (100% Swiss) is planned to be among the first instruments.
d. Switzerland is represented at ESS by Dr. Marc Janoschek (PSI) in the group for instrumentation, and Henrik Ronnow has been nominated to be the Swiss member in the Scientific Advisory Board of ESS.

11. News from SINQ (M. Kenzelmann)

a. Due to the long shutdown of SINQ until beginning of July 2018, there was only one call for proposals in Feb. 2018 for all instruments of SINQ. In addition, a second call for a few instruments was launched in summer 2018. Overall, a good number of proposals was received.
b. The commissioning of the new spectrometer CAMEA was started in November 2018 with fast progress. CAMEA is planned to be fully operational before the shutdown in December 2018.
c. The timeline of the SINQ upgrade remains unchanged. SINQ will be shut down in 2019 for the exchange of the neutron guides and work in the neutron bunker. The commissioning of the instruments with minor upgrade (FOCUS, TASP, SANS-I, Rita-2/CAMEA) is planned for January and February 2020. The second commissioning phase for AMOR, DMC, SANS-LLB and the instruments Orion and Narziss is planned to follow later in 2020.
d. In addition to the previous plans for the SINQ upgrade, the spectrometer Morpheus is now also planned to be upgraded in collaboration with Forschungszentrum Karlsruhe to become a 3-axis instrument. It is not planned to include Morpheus in the user program.

12. Name change of the society

In 2016, it was proposed to change the name of the Swiss Neutron Scattering Society to Swiss Neutron Science Society to reflect the openness for all researchers using neutrons. At the general assembly 2017, a vote about the new name was postponed, because arguments against the new name had been brought forward.

The board has opened an online discussion board about the new name, which was used by only two members of the society. It was mentioned that all activities needing access to neutron sources should be included in our Society and that it should not be necessary that researchers with interests in science using neutrons need to join several organisations.

In a discussion about the new name, it is mentioned that the name should be given at least in English, German and French.
A vote is taken, and the new name “Swiss Neutron Science Society (SNSS)” / “Schweizerische Gesellschaft für Neutronenforschung (SGN)” / “Société Suisse de la Science Neutronique (SSSN)” is accepted without a dissentient vote.

Miscellaneous

The contents and format of the newsletter of the Society, Swiss Neutron News, is discussed. It is proposed that the printed Swiss Neutron News could be replaced with a newsletter that is circulated by email. A reduction from two to one issue per year is also discussed. M. Strobl and Ch. Rüegg mention that Swiss Neutron News is a good advertisement for the Society and that it should have two issues per year. H. Ronnow has the feeling that Swiss Neutron News in its paper form is read and that the printed format is an advantage against the many newsletters that are sent out by email.
The board agrees to discuss the format and contents of Swiss Neutron News, and all members are invited to give their input for changes of Swiss Neutron News.

U. Gasser
January 2019

Conferences and Workshops 2019 and beyond

An updated list with online links can be found here:
http://www.psi.ch/useroffice/conference-calendar

May 2019

24th Annual Structural Biology Symposium
May 4, 2019, Galveston Island, USA

Gordon Research Seminar: Synergy of Neutron Scattering and Complementary Tools to Reveal New States of Matter
May 4-5, 2019, Hong Kong, CN

Gordon Research Conference: Emerging Neutronic Approaches for Advanced Materials Study and Innovation in Energy, the Environment, Health and Infrastructure
May 5-10, 2019, Hong Kong, CN

RapiData 2019 at SSRL - Data Collection and Structure Solving: A Practical Course in Macromolecular X-Ray Diffraction Measurement
May 5-10, 2019, Menlo Park, CA, USA

CETS 2019: 13th Central European Training School on Neutron Techniques
May 5-10, 2019, Budapest, Hungary

EGI Conference 2019
May 6-8, 2019, Amsterdam, The Netherlands

Cryo-EM Data Processing Workshop
May 6-9, 2019, Galveston, USA

PPXRD-16 and SPS-XRPD: Spring Pharmaceutical Synchrotron X-ray Powder Diffraction Workshop
May 9-12, 2019, PSI Villigen, Switzerland

RIPATHWAYS Workshop on Socioeconomic Impact of Research Infrastructures
May 10, 2019, Barcelona, Spain

French-Swedish school on X-rays and Neutrons techniques for the study of functional materials for energy
May 13-17, 2019, Lund, Sweden

Advanced Workshop on Cryo-Electron Tomography
May 13-17, 2019, Vienna, Austria

iNEXT course: X-ray and neutron crystallography: from data collection to structures
May 13-17, 2019, Oulu, Finland

Current trends and future of crystallography
May 14, 2019, Prague, Czech Republic

2nd Annual Industrial Biostructures America
May 19-21, 2019, San Diego, US

CNIO Frontiers Meeting. Structural and molecular biology of the DNA damage response
May 20-22, 2019, Madrid, Spain

Instruct Biennial Structural Biology Conference
May 22-24, 2019, Alcalá de Henares (near Madrid), Spain

7th International School on Biological Crystallization
May 26-31, 2019, Granada, Spain

Biology at different scales, an interplay between physics and biology
May 27 - June 7, 2019, Chamonix, France

Modern Cryo-Electron Microscopy. An international school
May 30 - June17, 2019, Dolgoprudny, Moscow Region, Russia

2019 International School of Crystallography
May 31 - June 9, 2019, Erice, Sicily, Italy

June 2019

14th International Symposium on Macrocyclic and Supramolecular Chemistry
June 2-6, 2019, Lecce, Italy

HAXPES 2019: 8th International Conference on Hard X-ray Photoelectron Spectroscopy
June 2-7, 2019, Paris, France

Summer School on Mathematical Crystallography
June 3-7, 2019, Nancy, France

International Soft Matter Conference
June 3-7, 2019, Edinburgh, UK

SNS/HFIR 2019 Neutron Scattering User Meeting
June 4-5, 2019, Oak Ridge National Laboratory, Tennessee, USA

MLZ Conference 2019: Neutrons for information and quantum technologies
June 4-7, 2019, Lenggries, Germany

HANDS 2019: HFIR/SNS Advanced Neutron Diffraction and Scattering Workshop
June 9-14, 2019, Oak Ridge National Laboratory, Tennessee, USA

The Zurich School of Crystallography 2019: Bring Your Own Crystals
June 16-27, 2019, Zürich, Switzerland

2019 National School on Neutron and X-ray Scattering
June 16-29, 2019, Argonne IL and Oak Ridge TN, USA

Bilbao Neutron School BNS 2019: Science and Instrumentation for Compact Accelerator-driven Neutron Sources (CANS)
June 17-19, 2019, Leioa - Vizcaya (Spain)

PSI Master School: Introducing photons, neutrons and muons for condensed matter physics and materials characterization
June 17-21, 2019, PSI Villigen, Switzerland

Open SESAME Environmental Science Thematic School
June 23-27, 2019, Allan, Jordan

ANSTO-HZB Neutron School
June 23-28, 2019, Lucas heights, Australia

International Symposium on Structure Biology for Drug Discovery at SwissFEL
June 25-27, 2019, PSI Villigen, Switzerland

Nanotech France 2019
June 26-28, 2019, Lucas heights, Australia

July 2019

ECNS 2019: European Conference on Neutron Scattering 2019
July 1-5, 2019, St Petersburg, Russia

MaThCryst: Second Shanghai International School
July 1-7, 2019, Shanghai, China

UCANS-8: 8th International Meeting of the Union for Compact Accelerator-driven Neutron Sources
July 8-11, 2019, Paris, France

DMI-2019: International Workshop on Dzyaloshinskii-Moriya Interaction and Exotic Spin Structures
July 8-12, 2019, St Petersburg, Russia

ISSCG-17: The 17th International Summer School on Crystal Growth
July 8-26, 2019, Boulder, Co, USA

ICMF: International Conference on Magnetic Fluids
July 8-12, 2019, Paris, France

ISSCG-17: The 17th International Summer School on Crystal Growth
July 21-27, 2019, Colorado, USA

2019 CHRNS Summer School on the Fundamentals of Neutron Scattering - Spectroscopy
July 22-26, 2019, Gaithersburg, MD, USA

Magnonics 2019
July 28 - August 1, 2019, Carovigno, Italy

Travelling Seminar 2019: Russian-German Summer School
July 28 - August 10, 2019, Lake Baikal to Moscow, Russia

August 2019

Racirir Summer School 2019: Structure, Real-time Dynamics and Processes in Complex Systems
August 4-11, 2019, Svetlogorsk, Russia

ICPS 2019: International Conference of Physics Students
August 10-17, 2019, Cologne, Germany

X-ray spectrometry - Satellite of ECM32
August 15-16, 2019, Vienna, Austria

International Advanced School in Muon Spectroscopy 2019
August 15-23, 2019, Rutherford Appleton Laboratory, Oxfordshire, UK

32nd European Crystallographic Meeting
August 18-23, 2019, Vienna, Austria

JEMS: Joint European Magnetic Symposia
August 26-30, 2019, Uppsala, Sweden

PHOTONICA2019: VII International School and Conference on Photonics
August 26-30, 2019, Belgrade, Serbia

European synchrotron and FEL user organisation (ESUO) Regional Workshop
August 28, 2019, Belgrade, Serbia

Traps in Mineralogy
August 31 - September 1, 2019, Perth, Australia

September 2019

17th ECSSC European Conference on Solid State Chemistry
September 1-4, 2019, Lille, France

DF8: Diffusion Fundamentals VIII
September 1-5, 2019, Erlangen, Germany

17th European School on Rheology
September 2-6, 2019, Leuven, Belgium

SISN Neutron Advanced School: Neutrons and Muons for Magnetism
September 2-6, 2019, Ispra, Italy

23rd Laboratory Course Neutron Scattering
September 2-13, 2019, Jülich and Garching, Germany

16th Oxford School on Neutron Scattering
September 2-13, 2019, Oxford, UK

ECIS Training Course Microfluidics and surface rheology
September 6-7, 2019, Leuven, Belgium

33rd ECIS Conference of the European Colloid and Interface Society
September 8-13, 2019, Leuven, Belgium

ECMS 2019: 9th European Conference on Mineralogy and Spectroscopy
September 11-14, 2019, Prague, Czech Republic

J-PARC 2019: 3rd J-PARC symposium
September 23-26, 2019, Tsukuba, Japan

October 2019

IX Congress of the Spanish Synchrotron User Association (AUSE) and the 4th ALBA User's Meeting
October 8-10, 2019, ALBA synchrotron facility, Spain

PSI 2019: Physics of Fundamental Symmetries and Interactions
October 21-25, 2019, PSI Villigen, Switzerland

SMS 2019: International Conference on Smart Materials and Surfaces
October 23-25, 2019, Lisbon, Portugal

SIPS 2019: Sustainable Industrial Processing Summit 2019
October 23-27, 2019, Cyprus

November 2019

LEAPS Plenary Meeting 2019
November 18-20, 2019, PSI Villigen, Switzerland

X-Rays and Matter
November 19-22, 2019, Villers-les-Nancy, France

December 2019

Symposium on Advanced Materials Exploration with Neutrons at the Materials Research Society (MRS) Fall Meeting 2019
Dezember 1-6, 2019, Boston, MA, USA

MLZ User Meeting 2019
Dezember 10-11, 2019, Garching, Germany

June 2020

LEAPS Conference
June 3-7, 2020, Elba, Italy

QENS/WINS 2020: 14th Conference on Quasielastic Neutron Scattering and 9th Workshop on Inelastic Neutron Spectrometers
June 8-12, 2020, San Sebastian, Spain

August 2020

PSI summer school on particle physics 2020August 9-15, 2020, Zuoz, Switzerland

Editorial

Editor
Swiss Neutron Science Society

Address
Sekretariat SGN/SSSN
c/o Paul Scherrer Institut
WLGA/018
5232 Villigen PSI, Switzerland
phone: +41 56 310 46 66
fax: +41 56 310 32 94
http://sgn.web.psi.ch

Bank Account
Postfinance: 50-70723-6 (BIC: POFICHBE)
IBAN: CH39 0900 0000 5007 0723 6

Printing
Paul Scherrer Institut
Circulation: 1600
2 numbers per year

Swiss Neutron Science Society
Sekretariat SGN/SSSN
WLGA/018
Paul Scherrer Institut
5232 Villigen PSI, Switzerland